Visual Neuroscience (2005), **22**, 275–281. Printed in the USA.

DOI: 10.1017/S0952523805223039

Channeling of red and green cone inputs to the zebrafish optomotor response

MICHAEL B. ORGER AND HERWIG BAIER

Department of Physiology, Program in Neuroscience, University of California—San Francisco, San Francisco

(RECEIVED December 22, 2004; ACCEPTED February 16, 2005)

Abstract

Visual systems break scenes down into individual features, processed in distinct channels, and then selectively recombine those features according to the demands of particular behavioral tasks. In primates, for example, there are distinct pathways for motion and form processing. While form vision utilizes color information, motion pathways receive input from only a subset of cone photoreceptors and are generally colorblind. To explore the link between early channeling of visual information and behavioral output across vertebrate species, we measured the chromatic inputs to the optomotor response of larval zebrafish. Using cone-isolating gratings, we found that there is a strong input from both red and green cones but not short-wavelength cones, which nevertheless do contribute to another behavior, phototaxis. Using a motion-nulling method, we measured precisely the input strength of gratings that stimulated cones in combination. The fish do not respond to gratings that stimulate different cone types out of phase, but have an enhanced response when the cones are stimulated together. This shows that red and green cone signals are pooled at a stage before motion detection. Since the two cone inputs are combined into a single 'luminance' channel, the response to sinusoidal gratings is colorblind. However, we also find that the relative contributions of the two cones at isoluminance varies with spatial frequency. Therefore, natural stimuli, which contain a mixture of spatial frequencies, are likely to be visible regardless of their chromatic composition.

Keywords: Cone photoreceptor; Motion vision; Psychopysics; Zebrafish

Introduction

Visually guided behaviors require the integration of many features of the visual environment, but the vertebrate retina starts by parsing a scene into separate features. Early on, photoreceptors sort by wavelength (Marks et al., 1964; Marc & Sperling, 1977), while bipolar cells sort increments and decrements of light (Werblin & Dowling, 1969). From behavioral and electrophysiological investigations, we can deduce that these channels are then used selectively in parts of the brain specialized for particular tasks (Livingstone & Hubel, 1988). A prominent example is human motion perception, which receives stronger inputs from long- (L) and middle-wavelength (M) cones than from short-wavelength (S) cones (Wandell et al., 1999). This could be explained by the fact that L and M cones greatly outnumber S cones in the primate retina (Marc & Sperling, 1977), and therefore provide more useful information about moving stimuli. Alternatively, there may be a deeper, ecological reason for the dominance of L and M cone inputs. Moving objects are defined by reflected light, which contains a smaller proportion of short wavelengths than direct light (Pichaud et al., 1999).

Address correspondence and reprint requests to: Herwig Baier, Department of Physiology, Program in Neuroscience, University of California—San Francisco, 1550 4th Street, Rock Hall, Room 348F, San Francisco, CA 94143-2722. E-mail: hbaier@itsa.ucsf.edu

In primates, a strong input to motion detection comes through a luminance channel that pools cone inputs. Chromatic inputs are much weaker, and may be processed through a distinct motion detection system (Lu et al., 1999). The reasons behind this filtering strategy are unclear. Perhaps, because trichromatic color vision is a relatively recent development in primates (Yokoyama & Radlwimmer, 2001), the motion pathway has not had enough evolutionary time to incorporate the new color-coding circuits, a reasonable explanation for primates, but not for fish and other vertebrates. Alternatively, a single, highly sensitive luminance channel may help to keep computation times short, increasing the likelihood of escaping predators or catching prey. If this is correct, we would expect a similar trend in the visual systems of phylogenetically diverse species. Indeed, the action spectra of motion detection by various animals, ranging from insects to vertebrates, are shifted toward longer wavelengths and lack color-opponent channels (Kaiser, 1974; Schaerer & Neumeyer, 1996), although these types of measurements cannot necessarily rule out contributions from less sensitive or less-abundant photoreceptor types.

In this paper, we have set out to investigate the computations that underlie motion processing by larval zebrafish. Zebrafish lend themselves to a comparative approach, because red/green color vision evolved independently in fish and primates (Nathans et al., 1986; Yokoyama & Radlwimmer, 2001), and there are striking differences in the organization of cones and of chromatic processing in the fish and primate retinas (Daw, 1967). We have employed

the fishes' innate tendency to swim with perceived motion, a reflex called the "optomotor response" (OMR), as an indicator of what moving stimuli zebrafish see in their environment (Orger et al., 2000; Maaswinkel & Li, 2003). Using stimuli targeting specific cone types (Chichilnisky et al., 1993), we find that in zebrafish, as in humans (Wandell et al., 1999; Ruppertsberg et al., 2003), motion detection is dominated by a luminance channel, which pools L and M cone signals. Although short-wavelength cones do not contribute to the OMR, they provide a major input to another visually guided swimming behavior, phototaxis. We further show that, while drifting sinusoidal gratings that equally stimulate both the L and M cones out of phase do not elicit an OMR, the cones' relative contributions to motion, and consequently their isoluminance ratios, vary with spatial frequency. Therefore, moving natural patterns, which contain multiple spatial frequencies, may always contain some luminance information.

Materials and methods

Fish rearing

Larvae were bred from crosses of adult TL strain zebrafish. They were raised on a 14:10 h light:dark cycle, with lights coming on at 8 AM. Behavioral testing always took place between 1 PM and 6 PM on day 7 postfertilization.

Movie design

Movies were created in Matlab, using the Psychophysics Toolbox extensions (Brainard, 1997; Pelli, 1997), and shown on a computer monitor (832 × 624 pixels, 75 Hz) using a Macintosh G3 computer. The spectral output of the monitor was measured using a CS-1000 spectroradiometer (Minolta, USA) at 1-nm intervals between 380 and 780 nm. The relative strength and gamma function of the three color channels was checked regularly with a LS-100 light meter (Minolta, USA). The cone sensitivities were estimated as in Hughes et al. (1998), and the sensitivity of each cone to each color channel was estimated by taking the scalar product of the cone sensitivity and the monitor's color channel spectrum. Since there are four cones and three monitor channels, we cannot find color directions isolating all of the cone types. However, after minimizing UV cone activation using a whole-screen filter, it was possible to find two color directions which isolated the red and green cones well, and a third which would only be visible to the blue and UV cones.

Movie presentation

For each experiment, 12 shallow, 305-mm long, acrylic tanks containing approximately 50 larvae each were placed on the screen. Before and after the presentation of each stimulus, still photographs of the tanks were taken using a Nikon Coolpix 3 Megapixel digital camera, controlled by Matlab *via* serial commands (Orger et al., 2004). All the sinusoidal gratings used in this study except in Figures 4C–4D have a wavelength of 56 mm and a temporal frequency of 0.93 Hz. The distribution of the fish was analyzed using custom macros in NIH Image. The difference in the average position of the fish after a rightward and a leftward presentation of a stimulus is a measure of the strength of that stimulus, which we call the optomotor index (OMI). The responses in this study are normalized to the response to the red cone grating in Fig. 1B, and an OMI of 1 therefore means that there is an average difference of 19.5 cm in the position of larvae after the two different presentations of a stimulus.

Results

To investigate which of the four cone photoreceptors provide input to the OMR, we created colored gratings designed to isolate specific cone types (Chichilnisky et al., 1993). Seven-day-old zebrafish have four cone types (Branchek & Bremiller, 1984), classified as red, green, blue, and UV sensitive (Nawrocki et al., 1985; Robinson et al., 1993), but rod function has not yet developed (Branchek, 1984). The four cones form an orderly mosaic (Branchek & Bremiller, 1984), so ratios of cone types are fixed from fish to fish, unlike primates (Marc & Sperling, 1977), and cone density is approximately uniform across the retina. We used three color directions, one targeting the red cones, one the green, and one for the blue and UV cones. Seven-day-old larvae respond vigorously to red and green cone-isolating gratings drifting across the computer monitor, but do not respond to blue/UV gratings (Figs. 1A & 1B). This shows that red/green double cones provide the dominant input to the OMR. This result is particularly striking in the light of observations that blue and UV cones are much more sensitive to light at this age than green or red cones, based on electroretinogram (ERG) measurements (Saszik et al., 1999).

The conclusion that the OMR is selective for particular visual channels would not be valid if functional blue and UV cone pathways did not exist at this age, or if the stimuli we used were not in fact visible to the fish. We have ruled out both of these possibilities by looking at cone inputs to another behavior, phototaxis. Stationary gradients (Fig. 1A) were presented to the fish, using the same colors and contrasts as the moving gratings in the previous experiment. The fish swim towards the brighter half of the screen for all three stimuli (Fig. 1C), demonstrating that the blue/UV-targeted stimulus is visible and can elicit a behavioral response from the fish.

While sinusoidal gratings are useful tools for analyzing motion responses, it is important to know whether the results we see hold for more diverse stimuli. Moving edges are a common feature of natural scenes, so we asked whether the fish would respond to isolated moving edges, using stimuli in which the screen changed from one color to another *via* a "wipe" (Fig. 2A). The edges were designed to be cone isolating, and were defined as *on* or *off* edges, depending on whether the light falling on the particular cone type was increased or decreased after the edge had passed. After the edge had passed across the screen, the movie repeated. Obviously, such a movie contains both *on* and *off* components, but motion direction is only conveyed through one channel. The output of the cones in the retina is transmitted through bipolar cells. Bipolar cells can be classified as *on* and *off* cells on the basis of their responses to increments and decrements of light (Werblin & Dowling, 1969). Having discovered which cones contribute to the OMR, we can ask whether both types of bipolar cells contribute.

Fig. 2B shows the responses of larvae to different *on* and *off* edges at the start of testing. The fish respond equally well to both red and green *on* and *off* edges at both time points, indicating that both *on* and *off* pathways contribute to the response. Initially, we also see responses to blue/UV *on* and *off* edges, although in opposite directions. Remarkably, the response to the *on* stimulus is in the opposite direction to stimulus motion. Because over time, in these wipe stimuli, one side of the screen is, on average, brighter than the other, just like the stationary gradients we used to assess

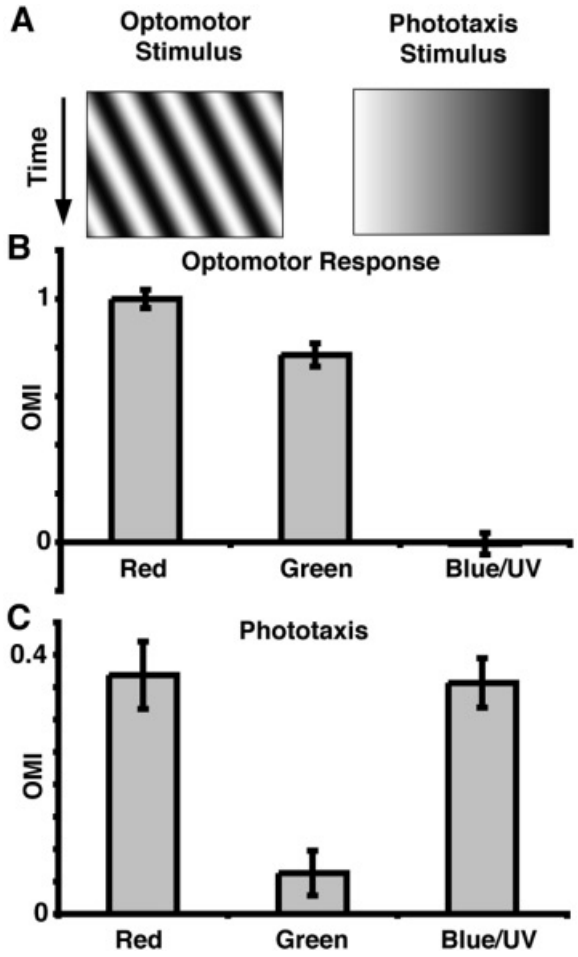

Fig. 1. Responses of zebrafish larvae to cone-isolating stimuli. (A) Time/space schematics of the stimuli used in this figure. On the left is a drifting sinusoidal grating, which elicits an OMR, and on the right is a stationary gradient that elicits phototaxis. (B) The distance swum by larvae in response to three cone-isolating sinusoidal gratings. Between each stimulus presentation the fish are brought back to the center of the tank by a high contrast converging sine-wave grating. The contrast in each case was calculated to be 70% for the isolated cone. A mean color was calculated for each case that allowed this contrast to be achieved. The error bars show standard error of the mean (SEM) (n = 9 batches of 25–50 fish). (C) Responses of larvae to stationary gradients using the same colors and contrasts as B. Stimuli are presented for 60 s. The fish swim towards the side of the screen which is brighter for the targeted cone type. The response is measured in the same manner as for the OMR, and expressed in terms of OMI. The error bars show SEM (n = 36).

phototaxis (see Fig. 1A), the response against the motion could be due to phototaxis. To distinguish between phototaxis and OMR, we took advantage of differences in response habituation. Larvae habituate rapidly to phototactic stimuli, giving robust responses initially, but giving no responses at all after just 10 min of testing. By contrast, the OMR shows little habituation over more than an hour of testing. This experiment confirmed a phototactic response towards the bluer side of the screen (Fig. 2C). After 10 min of testing, the short-wavelength responses have almost completely disappeared, while the red and green responses remain. The reason that the initial *on* response is weaker than the *off* response is that fish swimming with the direction of motion are exposed to the edge for longer than those swimming against it.

We have shown that red and green cone inputs dominate the OMR, but not how these cone inputs are combined. The different inputs could be pooled together, throwing out color information that could be extracted by comparing cone activations, or all information, including color, could be retained. A different experimental approach is required to distinguish between these probabilities.

We used a motion-nulling paradigm that had previously been used in human psychophysics (Chichilnisky et al., 1993). We classify gratings according to the ratio of the red, green, and blue cone contrasts, which we will call their 'color index.' If the grating stimulates two cone types out of phase, then the contrasts will be given opposite signs. Test gratings of different contrast, but with the same color index, are shown to the fish, superimposed on a fixed reference stimulus moving in the opposite direction (Fig. 3A). When the test contrast is low, then the fish swim in the direction of the reference grating, and when it is high, they follow the test grating (Fig. 3B). At some intermediate contrast the fish show no net movement, and the reference stimulus has been nulled. By finding nulling contrasts for test gratings with different color indices, we can find a set of gratings that have equivalent strength of input to the OMR. By plotting them graphically we can map a contour of equal OMR input strength in our three-dimensional stimulus space.

Red and green cones feed into the OMR to a similar degree: an 18.3% contrast green cone grating is equivalent in strength to a 16% contrast red cone grating (Fig. 3C). However, to match this strength with a blue/UV grating, a contrast of 66% is needed (Figs. 3D & 3E). This experiment uses near-threshold stimuli, which, even though presented for a whole minute, must be repeated many times to measure a significant response. Therefore, the practical contribution blue and UV cones make to the real-world OMR is negligible, as illustrated in Figure 1B. When red and green cone gratings are combined, the relative phase of the two is critical for the OMR (Fig. 3C). If the two gratings are in phase, the resulting combination is a stronger stimulus than either grating alone. However, when the gratings are combined out of phase, a weaker stimulus is produced. In fact, a grating with equal amounts of red and green cone contrast in opposite phase cannot reduce the response to the reference stimulus, even at the highest contrast we can show. In other words, for this stimulus set, OMR motion detection is colorblind. We conclude that red and green cone signals are pooled at an early stage before processing for visual motion.

The shape of these contours suggests that a single channel, consisting of pooled red and green cone signals, provides the dominant input to the OMR. A previous study investigating the response of adult zebrafish to a rotating striped drum illuminated by monochromatic light have concluded that only the red cone contributes to that response (Krauss & Neumeyer, 2003), and therefore it is important for us to verify that we really see multiple cone inputs in this system. We used two approaches to establish this: (1) differential adaptation of the cone inputs, and (2) measurement of the relative cone inputs at isoluminance across a range of stimulus parameters. If the stimuli were actually being sensed by just one cone type, then any kind of adaptation would affect responses to both red and green cone targeted stimuli in the same way. We adapted fish to a very bright or a very dim screen for 1 min before presenting OMR stimuli of varying brightness (Fig. 4A). We then compared the response of the fish in the bright and dim-adapted conditions. Unsurprisingly, the fish respond better to dim stimuli after adaptation to a dim screen, and better to bright stimuli after adaptation to a bright screen.

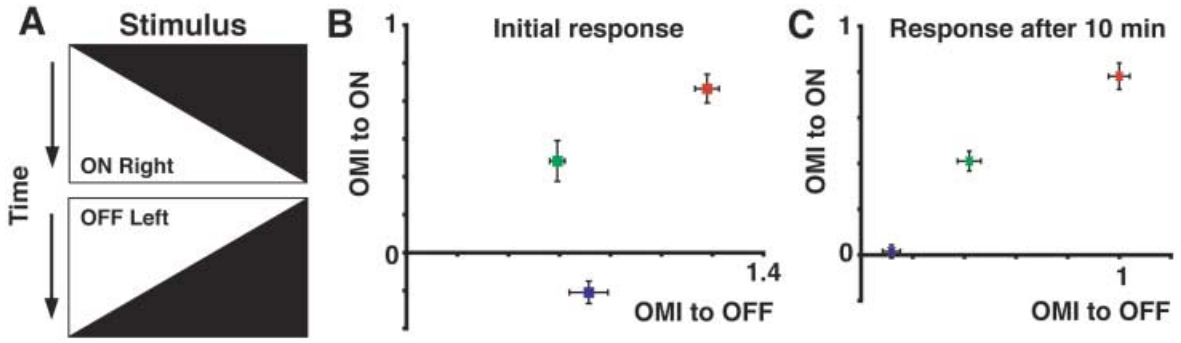

Fig. 2. Responses to *on* and *off* edges presented individually. *On* and *off* stimuli were presented for 60 s each. During each presentation the edge moved across the screen, until it reached the far end. The screen then reset to its original color and the edge started moving again. The process repeated at 0.125 Hz. The mean color and contrast of the edges was as in Fig. 1B. (A) Plots of space against time representing the *on* and *off* movies. The upper plot shows a white *on* movie moving to the right. The lower plot shows a white *off* movie moving to the left. (B) Responses to *on* and *off* edges in the first 5 min of testing. The graph shows the OMI of fish to *on* movies plotted against the same fishes' response to *off* movies. Red, green, and blue/UV cone isolating conditions are plotted as red, green, and blue points. Error bars show SEM ($n = 12$ tanks of 25–50 fish). (C) Responses to *on* and *off* edges after more than 10 min of testing. The graph shows the OMI of fish to *on* movies plotted against the same fishes response to *off* movies. Red, green, and blue/UV cone-isolating conditions are plotted as red, green, and blue points. Error bars show SEM ($n = 12$ tanks of 25–50 fish).

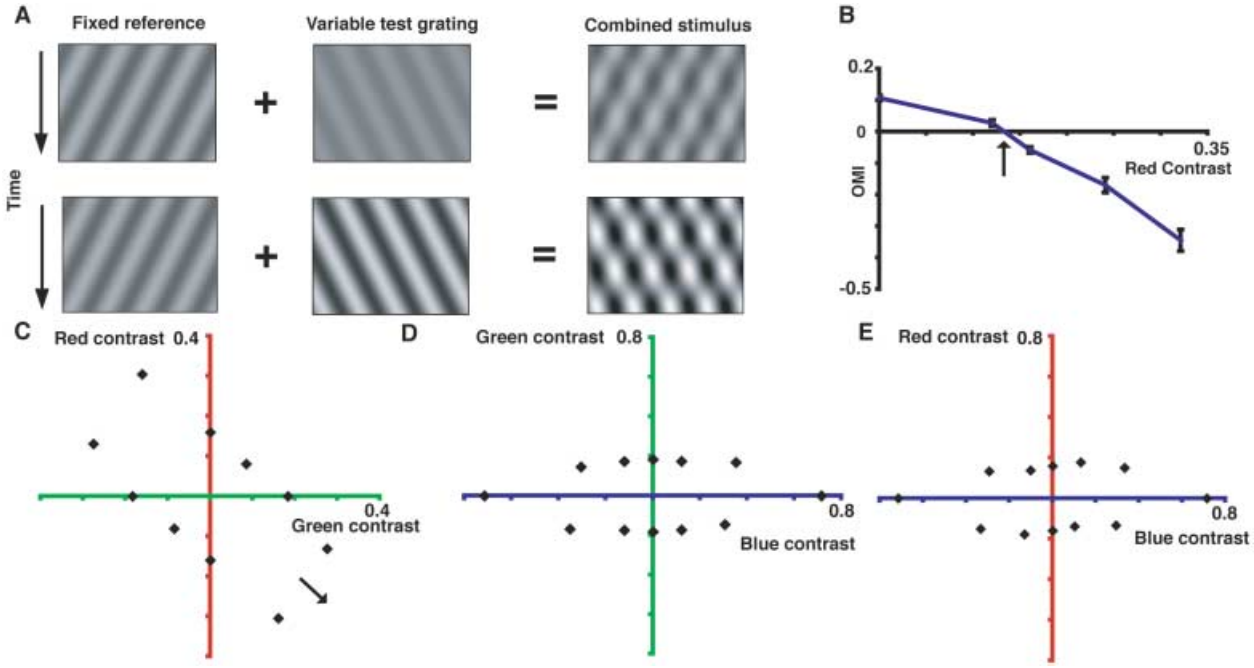

Fig. 3. Motion nulling identifies gratings with equivalent OMR input strength. (A) Schematic of the stimuli used. A reference grating with fixed contrast is superimposed on a test grating for which the contrast is varied. Each superimposed pair of stimuli are presented for 60 s. Several test contrasts are tried, and the null point is interpolated from the two data points nearest to the *x*-axis. (B) Example of the contrast-response function for one color direction (r:g:b/uv = 1:0:−3). Error bars show SEM ($n > 24$ batches of 25–50 fish each). At zero contrast, the fish swim with the reference grating, as indicated by the positive OMI ($0.11 \pm .007$; $n = 227$ tanks of 25–50 fish). As the test contrast gets higher the fish eventually reverse direction, with the null point calculated at 13.3% red contrast, as indicated by the arrow. (C) Points that null the reference grating in the red and green cone contrast plane. Every point in graphs C–E is derived from one experiment such as that shown in B. The distance of points from the origin reflects the contrast required to null the reference stimulus for that color direction. In one direction tested (r:g:b/uv = 1:−1:0, arrow), it is not possible to reduce the response to the reference grating with any test contrast, so no point is plotted for this direction. (D) In the green and blue/UV plane the contour is elongated along the blue axis. (E) In the red and blue/UV plane the contour is elongated along the blue axis.

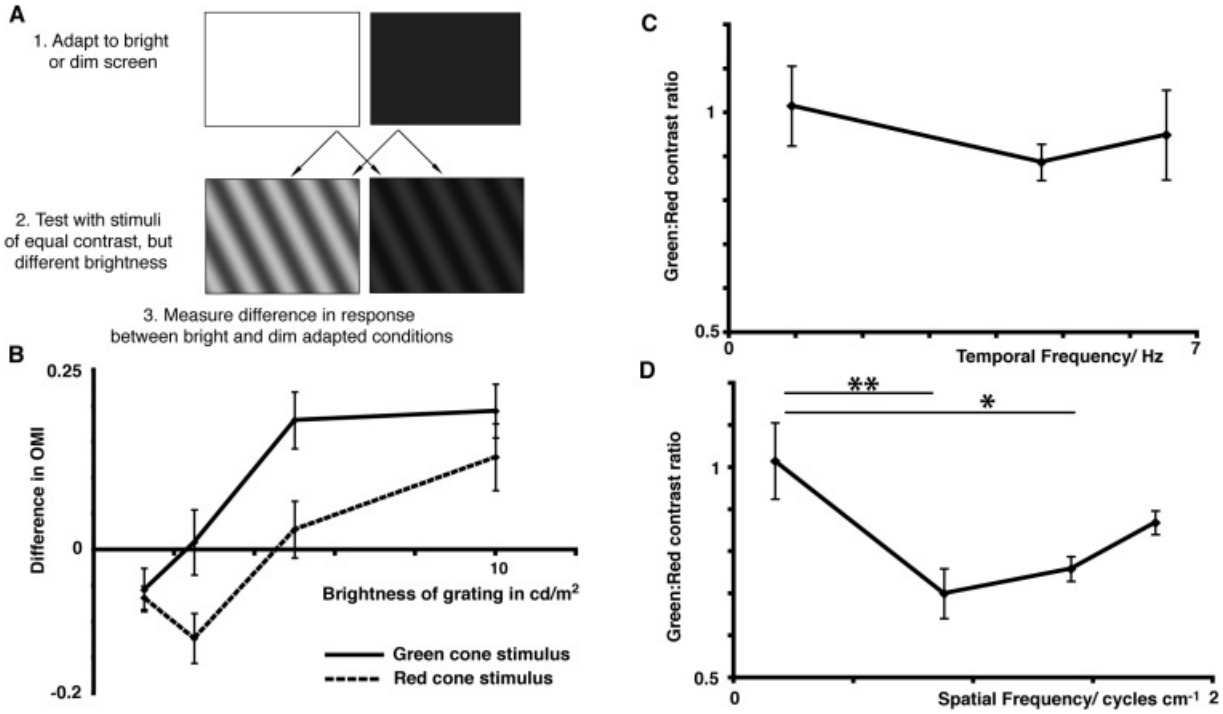

Fig. 4. Experimental evidence for the contribution of two cone types to the OMR. (A, B) Differential cone adaptation. (A) Experimental protocol: The optomotor response was tested after 1 min exposure to a bright screen (the monitor's green channel at full brightness, 55 cd/m^2) or a dim screen (one-eighth brightness). The optomotor response was tested using gratings isolating either red or green cones. The mean brightness of the OMR stimuli was varied over an eight-fold range, but the contrast and mean color were held constant. The response (OMI) to a particular grating after adaptation to a dim screen was subtracted from the response to the same grating after adaptation to a bright screen. (B) This difference in OMI is plotted as a function of OMR stimulus brightness, for the red (dashed line) and green (filled line) cone-isolating stimuli. Error bars show SEM ($n = 33$ batches of fish). (C, D) Relative red and green cone inputs at different spatial and temporal frequencies. Experimental protocol is as in Fig. 3. The reference stimulus is always a 12% contrast red cone-isolating grating, and the test stimuli are green cone-isolating gratings. Spatial and temporal frequency is varied for both the reference and test stimulus. (C) Ratio of red and green contrasts at the null point at different temporal frequencies. Spatial frequency is 0.18 cycles/cm. Errors bars show SEM ($n \geq 75$ batches of fish). (D) Ratio of red and green contrasts at the null point at different spatial frequencies. Temporal frequency is 0.93 Hz. Errors bars show SEM ($n \geq 113$ batches of fish). *Two-tailed t-test, $P < 0.02$. **$P < 0.01$.

In the adaptation experiment, stimuli of four different levels of brightness were used. The gratings shown were either red or green cone targeted. Figure 4B shows how the difference in response between the bright-adapted and dim-adapted conditions varies with stimulus brightness. As described above, the difference is positive for bright stimuli and negative for dim stimuli, for both red and green cone targeted gratings. However, the point at which the two curves cross the x-axis, that is, the point at which the response to the stimulus is the same for the two adaptation conditions, is clearly different. This can only be explained if the red and green cone gratings are really being detected by two separate cones.

The next experiment reinforces this observation in an intuitively simple way. If the red and green cone targeted stimuli that we are using were in fact being seen by only one cone, then the contrast required for a green cone targeted grating to null a red cone targeted grating of fixed contrast should be the same for all temporal and spatial frequencies. This is true for variations in temporal frequencies. Figure 4C shows that the ratio of red and green cone contributions at isoluminance does not vary significantly. However, this is not the case with changes in spatial frequency. We found that the relative contribution of green cones varied by up to 40% between different spatial frequencies (Fig. 4D), with a peak at intermediate frequencies. This implies that the cone inputs undergo some spatial filtering before they are pooled. Red cone inputs to motion detection are spatially more broadly tuned than green cone inputs.

This result has an interesting consequence for color and motion detection. The ratio of cone inputs to motion detections is what determines the slope of the contours shown in Figure 3C, and consequently which particular color direction will be invisible to the fish. If a stimulus contains multiple spatial frequencies, then this direction will be different for each component. Thus there will not be one color direction for which the motion of the stimulus is invisible.

Discussion

We have adapted a psychophysical approach, originally designed to probe human motion processing, to the study of the OMR in zebrafish larvae. The dominant input to the OMR comes through red and green cones. These cones come in closely associated pairs known as double cones (Robinson et al., 1995), which form an orderly mosaic in the zebrafish retina with blue and UV-sensitive cones. The magnitude of red and green cone contributions is similar, and both are much greater than the inputs

of blue/UV cones. This result does not reflect differences in maturity of the cones. First, other studies have found that contributions from shorter wavelength cones to the ERG *b*-wave reach mature sensitivity faster than contributions from longer wavelength cones (Saszik et al., 1999), and therefore, at 7 days postfertilization blue and UV cones are well developed and make functional connections. Second, we find that blue and/or UV cones provide a strong input to larval phototaxis. When the fish were shown whole-screen gradients using the same three color directions as the OMR experiments, the fish always swam towards the side of the screen which was brighter for the targeted cone. Populations of ganglion cells project to at least ten different brain areas in zebrafish (Burrill & Easter, 1994), providing an anatomical substrate for this channeling of selected features to different behaviors.

Why would two visual behaviors weight cone inputs in so dramatically different a way? The larval optomotor response is engaged by the apparent motion of the riverbed underneath the fish, which is normally perceived due to the pattern of reflected light (Rock & Smith, 1986). In our experiments, the fish swim to cancel the visual motion caused by an illusory current. By contrast, phototaxis is a response to direct light. Therefore, the different cone inputs might reflect the fact that direct light is richer in short wavelengths than reflected light (Pichaud et al., 1999). An ecological explanation that rests on properties of natural scenes is especially appealing when you consider how very different organisms weight spectral information similarly. Fish cones form an orderly mosaic and short-wavelength cones are present in roughly equal numbers to double cone pairs. By contrast, S cones in humans are found at relatively low density in most of the retina, and not at all in the fovea. However, short-wavelength cones provide weak contributions to motion processing in both fish and primates, lower than red and green inputs by four- (present study) to ten-fold (Seidemann et al., 1999), respectively.

Motion processing was further dissected by presenting individual moving edges. Moving edges arguably represent a more natural stimulus than a large-field drifting grating, and so it is important to show that such a stimulus can elicit a strong OMR, and that the cone contributions measured with moving edges are the same as those measured with gratings. By using isolated edges, we can also assess the relative contributions of *on* and *off* channels, an interesting question since we know that the neurons downstream of the cones, the bipolar cells, can be divided into *on* and *off* subtypes. Of course, bipolar cells do not carry exclusively *on* or *off* information, but *on* and *off* channels have been shown to carry distinct information about the visual scene. For example, *on* and *off* pathways convey different spectral information out of the retina (Wheeler, 1979) and thus could contribute selectively to specific behaviors. However, we found that *on* and *off* edges are equally well able to elicit an OMR.

It is interesting to compare this result with studies of the adult OMR in goldfish and zebrafish, which have found that the action spectrum of the response resembles that of red cone opsin, and concluded that only red cones contribute to the response (Schaerer & Neumeyer, 1996; Krauss & Neumeyer, 2003). Our study, looking at the larval response, concludes that both red and green cones contribute. We believe that our two experiments using differential adaptation and looking at differences in cone contributions at different spatial frequencies can only be explained by multiple cone inputs. This could, of course, simply reflect a real difference between larvae and adults, or between the experimental conditions used to elicit the response. The adult OMR is a response to a rotating drum surrounding the fish, and the larval OMR in this study is a response to drifting gratings presented from below. However, it is also likely to reflect a difference in the methods used to quantify cone input. The motion-nulling technique we use compares the contrast sensitivities of different cone inputs at a brightness well above threshold. Two cones with similar contributions measured in this way could still nonetheless have very different threshold sensitivities. Red cone sensitivity increases dramatically as the fish mature (Saszik et al., 1999) and may therefore come to dominate the action spectrum of the adult response.

We have compared the strength of various different gratings using a motion-nulling technique. This allows us to test the relative strength of gratings across a range of stimulus parameters. Importantly, since the technique involves finding stimuli to which the fish show no response, the results are largely independent of how well the fish can swim. This last point is important, because we can use these methods to probe visual processing even in mutants with mild swimming impairments. We find that a moving grating composed of alternating red and green stripes, which activates the red and green cones equally, but out of phase with each other, provides no input to the OMR (Fig. 3C). On the other hand, a grating with the same predicted red and green cone contrasts in phase (i.e. with red and green stripes superimposed) elicits a strong OMR. This finding shows that the response is, under these conditions, red/green colorblind. Moreover, the OMR to a red and a green cone grating superimposed in phase is greater than the response to either grating alone. This suggests that the two cone inputs are pooled into a single 'luminance' channel before motion detection. At what stage this pooling takes place is not clear. Red and green cones in the adult fish form closely associated double cones, which may indicate direct cone–cone connections. However, this double cone morphology is not apparent at the 7-day-old larval stage (Branchek & Bremiller, 1984).

How does this compare to motion detection in humans, whose red and green photopigments evolved independently from those in fish (Nathans et al., 1986; Yokoyama & Radlwimmer, 2001)? There have been decades of debate over the contribution of chromatic inputs to motion perception in primates (Zeki, 1977; Ramachandran & Gregory, 1978; Livingstone & Hubel, 1988; Cavanagh & Anstis, 1991; Hawken et al., 1994; Dougherty et al., 1999). Humans report that moving patterns of isoluminant red and green stripes appear to stand still. However, further studies have demonstrated that humans are able to detect motion of purely chromatic stimuli. Differences in the magnitude and parameters of the responses to luminance and chromatic stimuli have led to speculation that they are detected by different mechanisms, for example first- and third-order motion systems, respectively (Lu et al., 1999). Inputs to the fish OMR described here resemble the human first-order motion system. In a previous study (Orger et al., 2000), zebrafish larvae have also been shown to see second-order motion (which is devoid of luminance-modulated motion), but when they were shown a stimulus in which first-order luminance cues and third-order feature cues competed (Hammett et al., 1993), first-order cues clearly dominated the response.

In fish, just as in primates, when probed with a greater range of stimuli, the relationship between color and motion deviates from the simplified pictures of segregated streams. We show that the relative contribution of red and green cones varies with spatial frequency indicating that those inputs are spatially filtered before being pooled for motion detection. Changing the temporal frequency does not appear to affect the cone weights, perhaps because

temporal frequency sensitivity is limited by events within the photoreceptors (Baylor, 1996), whereas spatial-frequency processing must depend on integration, and hence filtering, by downstream cells in the inner retina or beyond. Since most natural stimuli, such as edges, contain a range of spatial frequencies, it is unlikely that many moving stimuli, outside the laboratory, will be completely invisible to the fish. Perhaps this and the relative simplicity of using a single channel for motion processing outweigh any disadvantage the fish may face by not being able to see some chromatic motion patterns. It will be an exciting challenge in the future to investigate the neural basis for these phenomena, using the many tools for genetic, physiological, and developmental analysis that have been developed in zebrafish (Gahtan & Baier, 2004).

Acknowledgments

H. Baier was supported by the grants from the following organizations: NIH RO1-EY12406, Packard Foundation, Klingenstein Foundation and the Sloan Foundation. M. Orger was supported by a Howard Hughes Medical Institute pre-doctoral fellowship. The authors would like to thank Wendy Staub and Liz Janss for providing more than 100,000 fish larvae and Megan Carey for helpful comments on the manuscript.

References

Baylor, D. (1996). How photons start vision. *Proceedings of the National Academy of Sciences of the U.S.A.* **93**, 560–565.

Brainard, D.H. (1997). The Psychophysics Toolbox. *Spatial Vision* **10**, 433–436.

Branchek, T. (1984). The development of photoreceptors in the zebrafish, brachydanio rerio. II. Function. *Journal of Comparative Neurology* **224**, 116–122.

Branchek, T. & Bremiller, R. (1984). The development of photoreceptors in the zebrafish, Brachydanio rerio. I. Structure. *Journal of Comparative Neurology* **224**, 107–115.

Burrill, J.D. & Easter, S.S., Jr. (1994). Development of the retinofugal projections in the embryonic and larval zebrafish (Brachydanio rerio). *Journal of Comparative Neurology* **346**, 583–600.

Cavanagh, P. & Anstis, S. (1991). The contribution of color to motion in normal and color-deficient observers. *Vision Research* **31**, 2109–2148.

Chichilnisky, E.J., Heeger, D. & Wandell, B.A. (1993). Functional segregation of color and motion perception examined in motion nulling. *Vision Research* **33**, 2113–2125.

Daw, N.W. (1967). Goldfish retina: Organization for simultaneous color contrast. *Science* **158**, 942–944.

Dougherty, R.F., Press, W.A. & Wandell, B.A. (1999). Perceived speed of colored stimuli. *Neuron* **24**, 893–899.

Gahtan, E. & Baier, H. (2004). Of lasers, mutants, and see-through brains: Functional neuroanatomy in zebrafish. *Journal of Neurobiology* **59**, 147–161.

Hammett, S.T., Ledgeway, T. & Smith, A.T. (1993). Transparent motion from feature- and luminance-based processes. *Vision Research* **33**, 1119–1122.

Hawken, M.J., Gegenfurtner, K.R. & Tang, C. (1994). Contrast dependence of colour and luminance motion mechanisms in human vision. *Nature* **367**, 268–270.

Hughes, A., Saszik, S., Bilotta, J., Demarco, P.J., Jr. & Patterson, W.F., II (1998). Cone contributions to the photopic spectral sensitivity of the zebrafish ERG. *Visual Neuroscience* **15**, 1029–1037.

Kaiser, W. (1974). The spectral sensitivity of the honey bee's optomotor walking response. *Journal of Comparative Physiology* **90**, 405–408.

Krauss, A. & Neumeyer, C. (2003). Wavelength dependence of the optomotor response in zebrafish (Danio rerio). *Vision Research* **43**, 1273–1282.

Livingstone, M. & Hubel, D. (1988). Segregation of form, color, movement, and depth: Anatomy, physiology, and perception. *Science* **240**, 740–749.

Lu, Z.L., Lesmes, L.A. & Sperling, G. (1999). The mechanism of isoluminant chromatic motion perception. *Proceedings of the National Academy of Sciences of the U.S.A.* **96**, 8289–8294.

Maaswinkel, H. & Li, L. (2003). Spatio-temporal frequency characteristics of the optomotor response in zebrafish. *Vision Research* **43**, 21–30.

Marc, R.E. & Sperling, H.G. (1977). Chromatic organization of primate cones. *Science* **196**, 454–456.

Marks, W.B., Dobelle, W.H. & Macnichol, E.F., Jr. (1964). Visual pigments of single primate cones. *Science* **143**, 1181–1183.

Nathans, J., Thomas, D. & Hogness, D.S. (1986). Molecular genetics of human color vision: The genes encoding blue, green, and red pigments. *Science* **232**, 193–202.

Nawrocki, L., BreMiller, R., Streisinger, G. & Kaplan, M. (1985). Larval and adult visual pigments of the zebrafish, Brachydanio rerio. *Vision Research* **25**, 1569–1576.

Orger, M.B., Gahtan, E., Muto, A., Page-McCaw, P., Smear, M.C. & Baier, H. (2004). Behavioral screening assays. *Methods in Cell Biology* **77**, 53–68.

Orger, M.B., Smear, M.C., Anstis, S.M. & Baier, H. (2000). Perception of Fourier and non-Fourier motion by larval zebrafish. *Nature Neuroscience* **3**, 1128–1133.

Pelli, D.G. (1997). The VideoToolbox software for visual psychophysics: transforming numbers into movies. *Spatial Vision* **10**, 437–442.

Pichaud, F., Briscoe, A. & Desplan, C. (1999). Evolution of color vision. *Current Opinion in Neurobiology* **9**, 622–627.

Ramachandran, V.S. & Gregory, R.L. (1978). Does colour provide an input to human motion perception? *Nature* **275**, 55–56.

Robinson, J., Schmitt, E.A. & Dowling, J.E. (1995). Temporal and spatial patterns of opsin gene expression in zebrafish (Danio rerio). *Visual Neuroscience* **12**, 895–906.

Robinson, J., Schmitt, E.A., Harosi, F.I., Reece, R.J. & Dowling, J.E. (1993). Zebrafish ultraviolet visual pigment: Absorption spectrum, sequence, and localization. *Proceedings of the National Academy of Sciences of the U.S.A.* **90**, 6009–6012.

Rock, I. & Smith, D. (1986). The optomotor response and induced motion of the self. *Perception* **15**, 497–502.

Ruppertsberg, A.I., Wuerger, S.M. & Bertamini, M. (2003). The chromatic input to global motion perception. *Visual Neuroscience* **20**, 421–428.

Saszik, S., Bilotta, J. & Givin, C.M. (1999). ERG assessment of zebrafish retinal development. *Visual Neuroscience* **16**, 881–888.

Schaerer, S. & Neumeyer, C. (1996). Motion detection in goldfish investigated with the optomotor response is "color blind". *Vision Research* **36**, 4025–4034.

Seidemann, E., Poirson, A.B., Wandell, B.A. & Newsome, W.T. (1999). Color signals in area MT of the macaque monkey. *Neuron* **24**, 911–917.

Wandell, B.A., Poirson, A.B., Newsome, W.T., Baseler, H.A., Boynton, G.M., Huk, A., Gandhi, S. & Sharpe, L.T. (1999). Color signals in human motion-selective cortex. *Neuron* **24**, 901–909.

Werblin, F.S. & Dowling, J.E. (1969). Organization of the retina of the mudpuppy, Necturus maculosus. II. Intracellular recording. *Journal of Neurophysiology* **32**, 339–355.

Wheeler, T.G. (1979). Retinal ON and OFF responses convey different chromatic information to the CNS. *Brain Research* **160**, 145–149.

Yokoyama, S. & Radlwimmer, F.B. (2001). The molecular genetics and evolution of red and green color vision in vertebrates. *Genetics* **158**, 1697–1710.

Zeki, S.M. (1977). Colour coding in the superior temporal sulcus of rhesus monkey visual cortex. *Proceedings of the Royal Society B* (London) **197**, 195–223.